

Identification of Novel Farnesyl Protein Transferase Inhibitors Using Three-Dimensional Database Searching Methods

James J. Kaminski,* D. F. Rane, Mark E. Snow, Lois Weber, Marnie L. Rothofsky, Samantha D. Anderson, and Stanley L. Lin

Schering-Plough Research Institute, Kenilworth, New Jersey 07033

Received May 5, 1997[⊗]

Generation of a three-dimensional pharmacophore model (hypothesis) that correlates the biological activity of a series of farnesyl protein transferase (FPT) inhibitors, exemplified by the prototype 1-(4-pyridylacetyl)-4-(8-chloro-5,6-dihydro-11*H*-benzo[5,6]cyclohepta[1,2-*b*]pyridin-11-ylidene)piperidine, Sch 44342, **1**, with their chemical structure was accomplished using the three-dimensional quantitative structure–activity relationship (3D-QSAR) software program, Catalyst. On the basis of the *in vitro* FPT inhibitory activity of a training set of compounds, a five-feature hypothesis containing four hydrophobic and one hydrogen bond acceptor region was generated. Using this hypothesis as a three-dimensional query to search our corporate database identified 718 compounds (hits). Determination of the *in vitro* FPT inhibitory activity using available compounds from this “hitlist” identified five compounds, representing three structurally novel classes, that exhibited *in vitro* FPT inhibitory activity, $IC_{50} \leq 5 \mu\text{M}$. From these three classes, a series of substituted dihydrobenzothiophenes was selected for further structure–FPT inhibitory activity relationship studies. The results from these studies is discussed.

Introduction

Ras proteins play an important role in signal transduction processes involved in cell proliferation and mutated constitutively activated ras proteins have been found in thirty percent of human cancers.^{1–3}

p21 Ras proteins (H, K, and N) are small guanine nucleotide binding proteins that undergo a series of posttranslational modifications which include the prenylation of ras by farnesyl protein transferase (FPT).^{4,5} These posttranslational modifications promote cell membrane association of ras which is necessary for its biological activity, e.g. cell growth and tumorigenesis. Realization that inhibition of ras farnesylation may offer therapeutic opportunities for the treatment of cancer has prompted significant effort to discover potent inhibitors of FPT as novel anticancer agents.^{6–8} Unfortunately, most of the FPT inhibitors reported to date are either peptide (peptidomimetic) in nature or contain metabolically sensitive functionality, i.e. free amino and/or sulfhydryl groups.

Discovery of the “tricyclic” FPT inhibitor 1-(4-pyridylacetyl)-4-(8-chloro-5,6-dihydro-11*H*-benzo[5,6]cyclohepta[1,2-*b*]pyridin-11-ylidene)piperidine, Sch 44342, **1**, was reported recently, Figure 1.⁹ Sch 44342, **1**, is a unique example of a novel nonpeptide, nonsulfhydryl-containing FPT inhibitor that exhibits substantial selectivity against geranyl geranyltransferase-1 (GGPT-1), and kinetically competes with the ras protein, but not with farnesyl pyrophosphate (FPP), in binding to FPT. Significant effort has been expended to optimize the *in vitro* FPT inhibitory potency, and the *in vivo* pharmacologic profile of this series of FPT inhibitors by conducting a systematic structure–FPT inhibitory activity relationship (SAR) study directed by chemical synthesis.^{10–12} Concomitant with this effort has been an analysis of the FPT inhibitory activity data determined *in vitro* for these

compounds using the three-dimensional quantitative structure–activity relationship (3D-QSAR) software program Catalyst.^{10,13}

One application of this program is the generation of hypotheses that attempt to correlate the biological activity observed for a series of compounds to their chemical structure.¹⁴ The hypotheses generated are three-dimensional descriptions of a pharmacophore model proposed for the series of compounds examined. The hypotheses are represented by the chemical features that describe the series of compounds, e.g. hydrophobic groups, hydrogen bond donors, hydrogen bond acceptors, positive and negative ionizable groups, etc. The hypotheses generated may be used to estimate the biological activity of proposed targets allowing a rank ordering of synthetic priorities. In addition, the hypotheses generated may also be used as three-dimensional queries to search databases of proprietary and/or commercially available compounds. These three-dimensional searches could identify structurally novel analogues that might exhibit the biological activity of the prototype.

The results obtained from searching our corporate database using a Catalyst-generated FPT hypothesis as a three-dimensional query form the subject matter of this report.

Chemistry

Substituted Tricyclic FPT Inhibitors. From the analogues prepared to investigate the structure–FPT inhibitory activity relationship of the series exemplified by the prototype 1-(4-pyridylacetyl)-4-(8-chloro-5,6-dihydro-11*H*-benzo[5,6]cyclohepta[1,2-*b*]pyridin-11-ylidene)piperidine, Sch 44342, **1**,^{9–11} a training set of compounds was selected for Catalyst analysis, Figure 1.

Substituted Dihydrobenzothiophenes. The substituted dihydrobenzothiophenes described in Table 2 were prepared using methodology that has been published previously.¹⁵

* To whom correspondence should be addressed.

⊗ Abstract published in *Advance ACS Abstracts*, November 15, 1997.

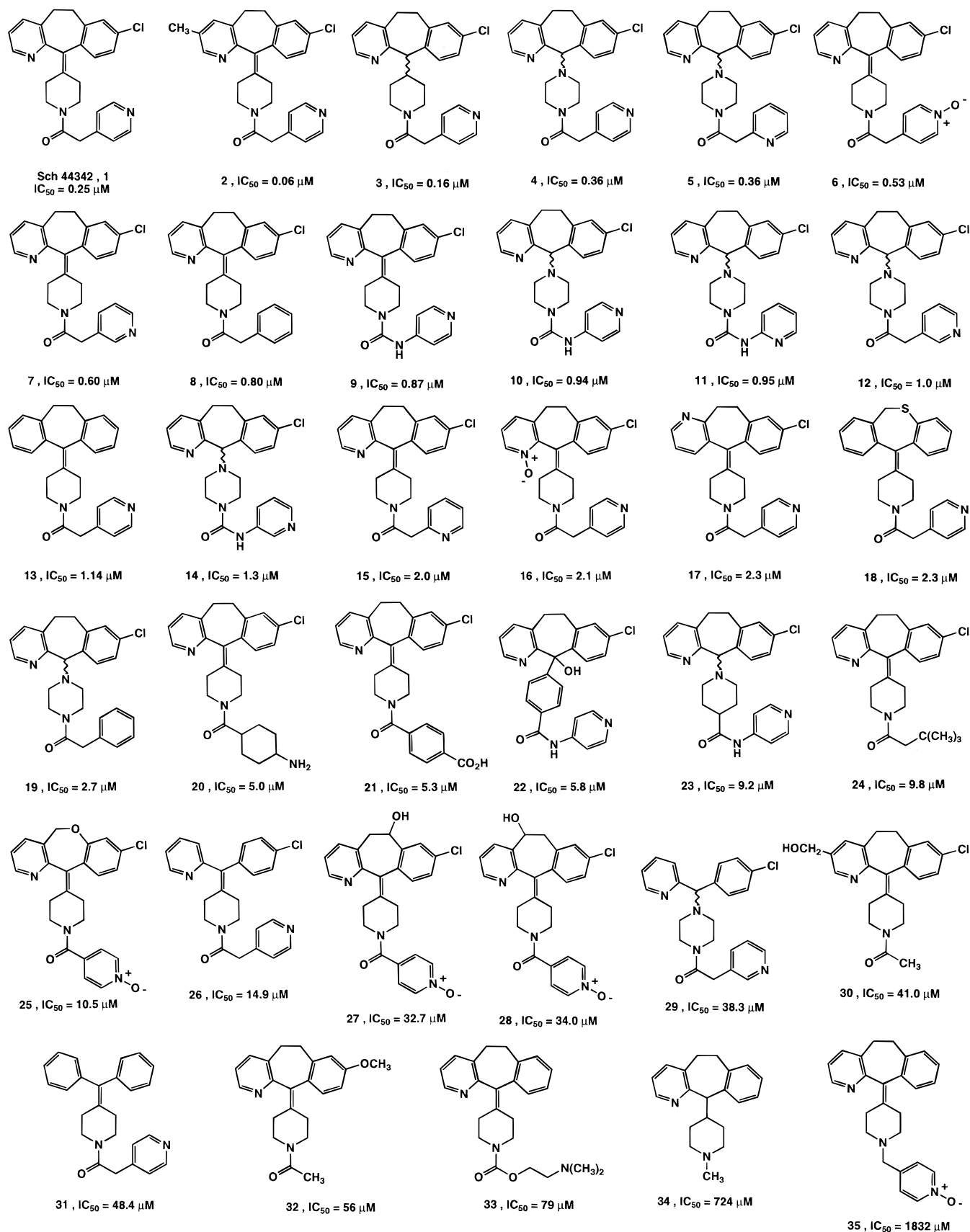


Figure 1. Training set of selected farnesyl protein transferase (FPT) inhibitors and their SPA-determined in vitro FPT inhibitory activity.

Biological Test Methods

In vitro Enzyme Assays of FPT and GGPT-1.
The in vitro FPT inhibitory activity of the compounds was evaluated using two assays (Table 2).

The primary FPT inhibitory assay was done using a scintillation proximity assay (SPA) kit following the protocol described by the manufacturer (Amersham) except that a biotinylated substrate peptide containing

Table 1. Comparison between the Measured and Estimated FPT Inhibitory Activity of the Catalyst Training Set

compd	FPT inhibitory activity		compd	FPT inhibitory activity	
	measured -log IC ₅₀	estimated -log IC ₅₀		measured -log IC ₅₀	estimated -log IC ₅₀
1	1.222	1.066	19	-0.431	-0.176
2	0.796	0.538	20	-0.699	-0.663
3	0.602	0.201	21	-0.724	-0.066
4	0.444	1.114	22	-0.763	-0.279
5	0.444	0.060	23	-0.964	-0.279
6	0.276	-0.114	24	-0.991	-0.146
7	0.222	0.319	25	-1.021	-1.633
8	0.097	0.000	26	-1.173	-0.447
9	0.060	0.222	27	-1.515	-1.763
10	0.027	-0.380	28	-1.531	-0.978
11	0.022	-0.079	29	-1.583	-0.813
12	0.000	-0.301	30	-1.613	-0.892
13	-0.057	-0.602	31	-1.685	-1.342
14	-0.114	-0.114	32	-1.748	-1.792
15	-0.301	-0.279	33	-1.898	-1.949
16	-0.322	-0.462	34	-2.860	-3.230
17	-0.362	-0.176	35	-3.263	-2.301
18	-0.362	-0.398			

the K-Ras carboxy terminal sequence was used.⁹ Initially, the FPT inhibitory activity of each compound was determined at a screening dose of 20 $\mu\text{g}/\text{ml}$. For those compounds that inhibited FPT by $\geq 50\%$ at the screening dose, an IC₅₀ was calculated from a dose-response curve by linear regression.

Alternatively as a secondary assay, the FPT inhibitory activity was determined by measuring transfer of [³H]farnesyl from [³H]farnesyl pyrophosphate to TCA-precipitable His₆-H-Ras-CVLS as described by Bishop et al.⁹

The GGPT-1 assay was essentially identical with the TCA precipitation assay for FPT described by Bishop et al.⁹ with two exceptions: [³H]geranyl geranylpyrophosphate (220–250 nM) replaced farnesyl pyrophosphate as the isoprenoid donor and H-Ras-CVLL (3.6 $\mu\text{g}/100 \mu\text{L}$ reaction) was the protein acceptor, similar to the method reported by Casey.¹⁶

Selectivity was expressed as the ratio of the GGPT-1 to FPT inhibitory activities (IC₅₀).

Computational Methods

FPT hypothesis creation and searching a database of compounds using the generated FPT hypothesis as a three-dimensional query was accomplished using Catalyst, version 2.1.¹³ Calculations were performed using a Silicon Graphics Challenge XL operating under IRIX 5.3.

Results and Discussion

From the analogues which were prepared to investigate the structure-FPT inhibitory activity relationships of this series, a training set of compounds was selected for Catalyst analysis, Figure 1. The compounds in the training set included the most active FPT inhibitors in the series, and each compound possessed something new to teach Catalyst during hypothesis generation. In addition, the compounds in the training set were structurally distinct from a chemical feature point of view and represented the diversity of the series. Each compound in the training set was considered as a collection of energetically reasonable conformations, and in cases where the chirality of an asymmetric center was not specified, Catalyst-generated and considered alternative stereoisomers.

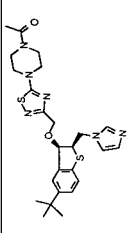
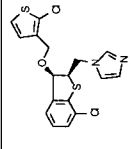
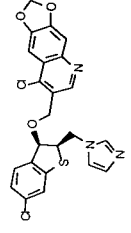
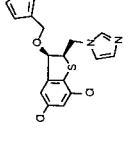
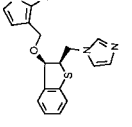
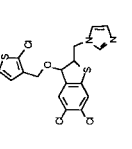
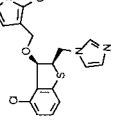
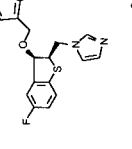
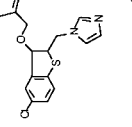
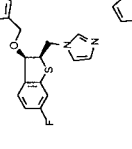
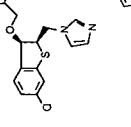
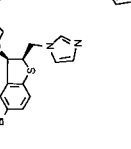
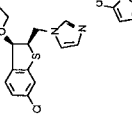
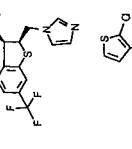
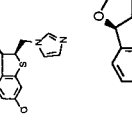
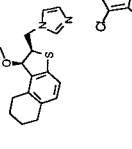

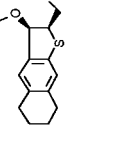
The range of in vitro FPT inhibitory activity exhibited by these selected compounds spanned 4 orders of magnitude, i.e. 10^{-1} – $10^3 \mu\text{M}$. Using this training set, FPT hypotheses (pharmacophore models) were generated. When generating hypotheses, Catalyst tries to minimize a cost function consisting of three terms. One term is a value that increases in a Gaussian form as the feature weight in a model deviates from an idealized value of two, i.e. the weight cost. The second term penalizes the deviation between the estimated activities of the training set and their experimentally determined values, i.e. the error cost. The third term penalizes the complexity of the hypothesis, i.e. the configuration cost. This is a fixed cost which is equal to the entropy of the hypothesis space. The overall cost of a hypothesis is calculated by summing over the three cost factors. Of these three, the error cost contributes the most in determining the cost of a hypothesis. During hypothesis generation, Catalyst calculates the cost of two theoretical hypotheses, one in which the error cost is minimal, the slope of the activity correlation line is one, the ideal hypothesis, and one where the error cost is high, the slope of the activity correlation line is zero, the null hypothesis. The greater the difference between these two costs, the higher the probability of generating a useful model.

The FPT hypothesis chosen from the alternatives generated was that which exhibited the lowest cost value and resided closest to the ideal hypothesis, Figure 2.¹⁴ The FPT hypothesis is a collection of chemical features distributed in three-dimensional space that is intended to represent groups in the molecule that participate in important binding interactions between drugs and their receptors. The pharmacophore model produced consisted of four hydrophobic regions and one hydrogen bond acceptor site in a specific three-dimensional orientation. Each of the five features in this model were equally weighted. Using **2**, IC₅₀ = 0.06 μM , as an example, a flexible fit of the best conformer of this molecule maps to the lowest cost Catalyst-generated FPT hypothesis as described in Figure 2. The four hydrophobic regions of the hypothesis are the 3-methyl group on the pyridyl portion of the tricyclic system, the 5,6-ethano bridge of the tricyclic system, the aromatic ring of the 8-chlorophenyl portion of the tricyclic system, and the 4-pyridyl ring of the picolinamide attached to the pendent piperylidenyl ring. The hydrogen bond acceptor identified in the FPT hypothesis generated is the carbonyl group of the γ -picolinamide attached to the pendent piperylidenyl ring.

A regression line of "measured" versus "estimated" FPT inhibitory activity for the training set, expressed as $-\log \text{IC}_{50}$, based on the lowest cost Catalyst-generated FPT hypothesis exhibited a correlation coefficient (r^2) = 0.91, and a root-mean-square deviation rms = 0.84, Figure 3. Using these criteria, comparison between the "estimated" activity of the compounds in the training set relative to their experimentally observed activity is in the worst case, within 1 order of magnitude, and in most cases, is within a 5-fold difference, Table 1.

In cases where one chiral center is present in the molecule, the generated FPT hypothesis exhibits a preference for the *S*-stereoisomer relative to the *R*-stereoisomer, e.g. the "estimated" FPT inhibitory po-

Table 2

Cmpd	MOLSTRUCTURE	% Inhibition 20 μ g / ml	SPA - FPT IC50 (μ M)	GGPT-1 IC50 (μ M)	Selectivity	Cmpd	MOLSTRUCTURE	% Inhibition 20 μ g / ml	SPA - FPT IC50 (μ M)	GGPT-1 IC50 (μ M)	Selectivity
39		86	4.8	> 39	> 8	48		92	6		
40		69	2.5	1.4	0.6	49		86	1.6	16.2	10.1
41		94	1.1	46.8	42.5	50		93	1.4	2.9	2.1
42		89	1.3	36.5	28.1	51		95	1.8	34.1	18.9
43		92	2.5			52		91	13.6		
44		96	2.3			53		88	1.1	14.2	12.9
45		95	16			54		75	10.7		
46		89	2.5			55		90	0.2	16.8	84
47		88	2	5	2.5	56		61	10.8		

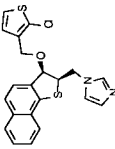
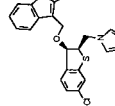
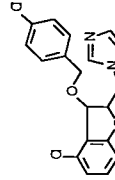
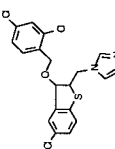
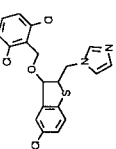
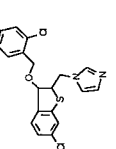
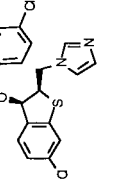
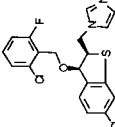
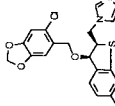
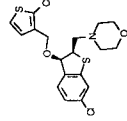
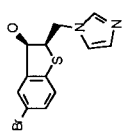
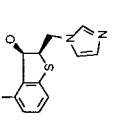
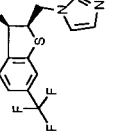
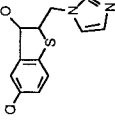
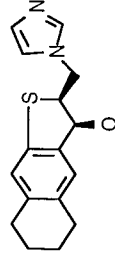
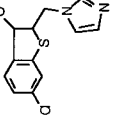
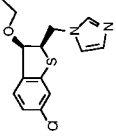
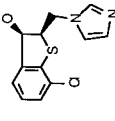
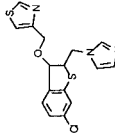
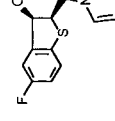
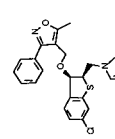
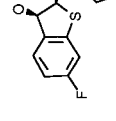
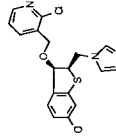
57		76	1.5	15	10	83	1.4	18.8	13.4
58		68	2	38	19	60	12.3		
59		95	1.3			90	2.7		
60		99	0.2	0.7	3.5	91	0.7	18.3	26.1
61		85	5.3			96	0.7	9.8	14
62		75	5.4			94	2.3		
63		95	1.2	12.9	10.8	79	20.8		
64		92	4.4			60	45.9		
65		80	3.2			30			

Table 2 (Continued)

Cmpd	MOLSTRUCTURE	% Inhibition 20 μ g / ml	SPA - FPT IC50 (μ M)	GGPT-1 IC50 (μ M)	Selectivity	Cmpd	MOLSTRUCTURE	% Inhibition 20 μ g / ml	SPA - FPT IC50 (μ M)	GGPT-1 IC50 (μ M)	Selectivity
75						82					
76		2				83		44			
77		14	266			84		42			
78			> 75			85			> 70		
79		58				86		88	8.5		
80		44				87		90	10.7		
81		23				88		90	2.5		
		38						95	1.3	3.3	2.5

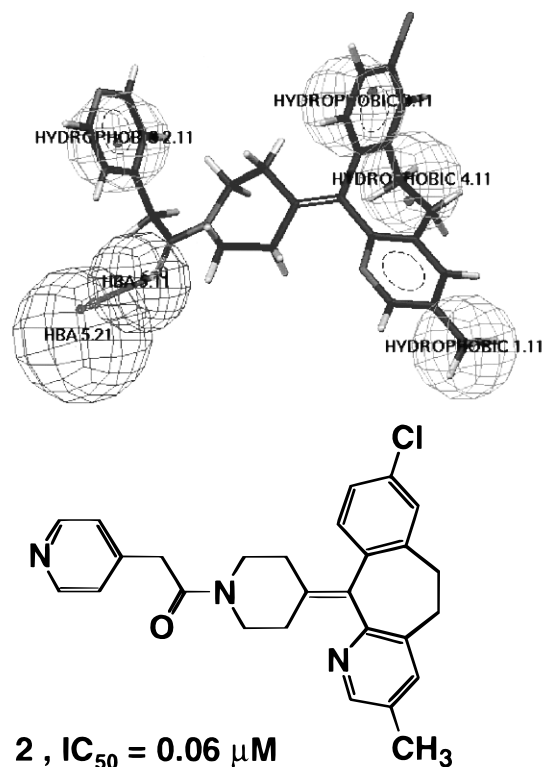


Figure 2. Best conformation of **2** flexibility fit to the lowest cost catalyst generated FPT hypothesis (pharmacophore model).

tency of the *S*(-)-stereoisomer of **4**, $IC_{50} = 0.014 \mu M$, is greater than the "estimated" FPT inhibitory potency of the *R*(+)-stereoisomer of **4**, $IC_{50} = 0.65 \mu M$. This observation is consistent with the "measured" FPT inhibitory potency determined for the enantiomers of **4**, the *S*(-)-stereoisomer, $IC_{50} = 0.14 \mu M$ relative to the *R*(+)-stereoisomer, $IC_{50} = 0.49 \mu M$.¹⁰ In general, this observation is consistent with the FPT inhibitory potency determined for enantiomers of several other analogues in the series, i.e. the *S*-stereoisomer exhibits a greater FPT inhibitory potency relative to the *R*-stereoisomer.

The FPT inhibitory activity predicted for compounds which were not part of the training set, but contain chemical features on which the FPT hypothesis was based, is usually within a 4–5-fold difference. However, consistent with other quantitative-structure activity relationship methods, activity predictions for compounds outside the training set are inaccurate and can be misleading, e.g. the "estimated" FPT inhibitory activity of the peptide CVWM, $IC_{50} = 0.007 \mu M$ is approximately 2 orders of magnitude different from its experimentally "measured" FPT inhibitory activity, $IC_{50} = 0.525 \mu M$.

The lowest cost Catalyst-generated FPT hypothesis was also used as a three-dimensional query to search the Schering-Plough Research Institute's corporate database and resulted in the identification of 718 compounds. Examination of these compounds revealed that 626 structures were unique, only 330 were available, and determination of their in vitro FPT inhibitory activity was initiated.

From the structures examined, only five compounds (5/330 = 1.5%) exhibited an in vitro FPT inhibitory potency $IC_{50} \leq 5 \mu M$, Figure 4. The 1.5% value obtained from this focused assessment of the corporate database

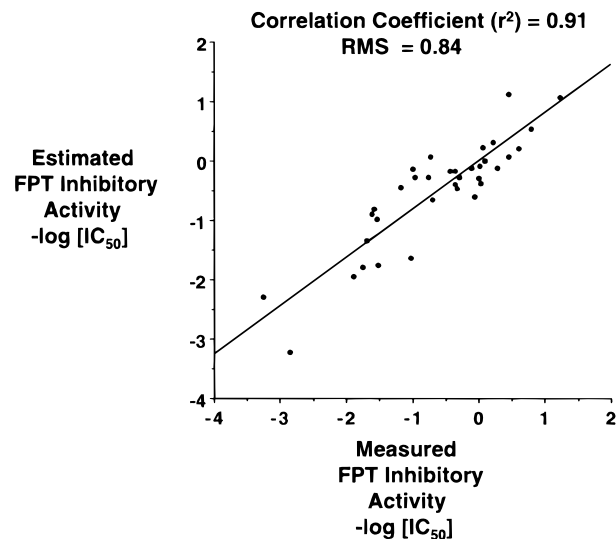


Figure 3. Comparison between the "measured" and "estimated" FPT inhibitory activity for the training set, expressed as $-\log IC_{50}$, based on the lowest cost catalyst generated FPT hypothesis.

is approximately a 2-fold improvement compared to determining the FPT inhibitory activity of a larger subset of the corporate database. High-throughput screening (HTS) of approximately 84 000 structures identified 2468 compounds which exhibited FPT inhibition $\geq 50\%$ at $20 \mu g/mL$. From these compounds, only 22 (22/2468 = 0.9%) exhibited an in vitro FPT inhibitory potency $IC_{50} \leq 5 \mu M$.

Of the five compounds identified, one is steroid-based, **36**, two are peptide-based, **37** and **38**, and two, **39** and **40**, are derived from a series of "azole" antifungals which were clinically investigated as topical agents.¹⁵

From a chemical point of view, the "azole" antifungals represent a novel class of FPT inhibitors that are structurally distinct from the "tricyclic" series of compounds, as well as other known FPT inhibitors. On that basis, the FPT and GGPT-1 inhibitory activities of these initial leads were profiled further.

The FPT inhibitory potency of **39** and **40** was independently confirmed using the secondary assay, i.e. the FPT inhibitory potency of **39** and **40** determined using the FPT Ras/TCA assay was $IC_{50} = 5.3 \mu M$ and $IC_{50} = 3.1 \mu M$, respectively. Selectivity between FPT and GGPT-1 inhibitory activity for **39** and **40** was also demonstrated, Table 2. In addition, the lack of significant FPT inhibitory activity exhibited by other "azole" antifungal agents, e.g. ketoconazole ($IC_{50} > 46 \mu M$) and fluconazole (% inhibition = 3 at $20 \mu g/mL$) suggested that the FPT inhibitory activity of these compounds may not be coupled to their antifungal activity. These observations encouraged us to determine the in vitro FPT inhibitory potency of other available analogues from this series.

Structure–FPT Inhibitory Activity Relationships

The in vitro FPT inhibitory data described in Table 2 suggested the following structure-activity relationships:

R₃ Substituent. Methodology utilized to prepare the synthetic intermediate alcohols, **76–84**, resulted in the preparation of only the *cis*-2,3-substituted stereoisomer.¹⁵ The presence of a lipophilic alkyloxy, or lipophilic

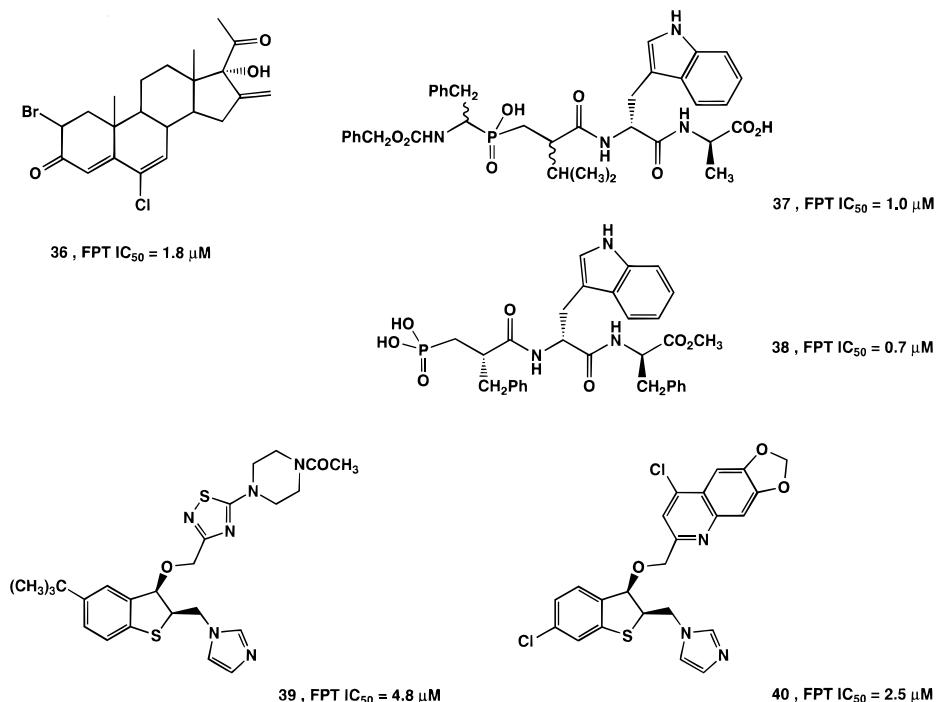


Figure 4. Novel compounds exhibiting in vitro FPT inhibitory activity $IC_{50} \leq 5 \mu M$ identified by searching the Schering-Plough Research Institute corporate database using the lowest cost catalyst generated FPT hypothesis.

arylalkyloxy or heteroarylalkyloxy group at the 3-position of the dihydrobenzothiophene ring system appears to be necessary to maintain in vitro FPT inhibitory activity.

While the intermediate alcohols **76–84** were devoid of significant FPT inhibitory activity, i.e. the % FPT inhibition ≤ 50 at $20 \mu g/mL$, or $IC_{50} > 50 \mu M$, introduction of halogen atoms at different positions in the aryl ring or heteroaryl ring of the 3-substituent resulted in more potent compounds. The FPT inhibitory potency of the 2-chloro(3-thienyl) analogue, **44**, $IC_{50} = 2.3 \mu M$, the 5-chloro(2-thienyl) analogue, **47**, $IC_{50} = 2 \mu M$, and the 2,5-dichloro(3-thienyl) analogue, **46**, $IC_{50} = 2.5 \mu M$, were each greater than the FPT inhibitory potency of the nonhalogenated (3-thienyl) analogue, **45**, $IC_{50} = 16 \mu M$.

In addition, the substitution pattern of the halogenated 3-arylalkyloxy substituent significantly influences the FPT inhibitory activity of the analogue. The FPT inhibitory potency of the 2,4-dichloro-substituted compound, **60**, $IC_{50} = 0.2 \mu M$, is greater than the FPT inhibitory potency of either the 2,6-dichloro-substituted compound, **61**, $IC_{50} = 5.3 \mu M$, or the monochloro-substituted compound, **59**, $IC_{50} = 16 \mu M$.

R₂ Substituent. Substitution in the imidazole ring, or replacement of the imidazole with an alternative amine resulted in the loss of FPT inhibitory activity for each analogue. Relative to the unsubstituted imidazole analogue **44**, $IC_{50} = 2.3 \mu M$, the FPT inhibitory activities of **74**, the 2-(hydroxymethyl)imidazole analogue, and **75**, the morpholino analogue, were less, i.e. % inhibition = 30 at $20 \mu g/mL$ and % inhibition = 2 at $20 \mu g/mL$, respectively.

Aromatic Substitution. Independently introducing chlorine at the 5-, 6-, 7-, and 8-position of the dihydrobenzothiophene ring system resulted in analogues **42**, **43**, **44**, and **48**, respectively. The FPT inhibitory activity of the 5-chloro-substituted analogue **42**, $IC_{50} = 1.3 \mu M$,

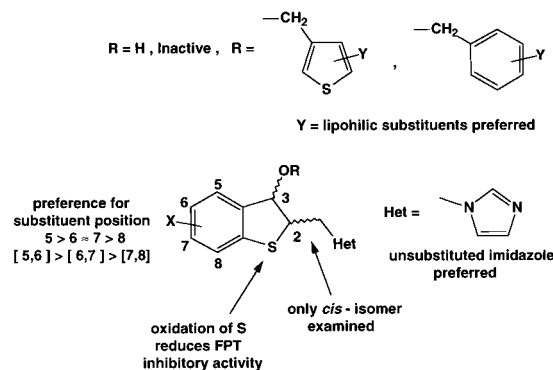


Figure 5. Preliminary structure–FPT inhibitory activity relationships of the substituted dihydrobenzothiophenes.

was essentially equivalent to the FPT inhibitory activity of the unsubstituted analogue **41**, $IC_{50} = 1.1 \mu M$.

Introduction of a 6-chlorine atom, **43**, $IC_{50} = 2.5 \mu M$, or a 7-chlorine atom, **44**, $IC_{50} = 2.3 \mu M$, did not significantly alter the FPT inhibitory potency of the analogue relative to **42** or **41**. However, introduction of an 8-chlorine atom significantly reduced the FPT inhibitory potency of the analogue, **48**, $IC_{50} = 6 \mu M$.

The deleterious effect of the presence of an 8-substituent on the FPT inhibitory potency of the analogue could be overcome by the presence of an additional substituent in the dihydrobenzothiophene ring system, i.e. the FPT inhibitory potency of the 6,8-dichlorosubstituted analogue, **49**, $IC_{50} = 1.6 \mu M$, is greater than the FPT inhibitory potency of the 8-chlorosubstituted analogue, **48**, $IC_{50} = 6 \mu M$, and comparable to the FPT inhibitory potency of the 6-chlorosubstituted analogue, **43**, $IC_{50} = 2.5 \mu M$.

Fusion of a cyclohexyl ring to the 5,6-positions, or the 6,7-positions of the dihydrobenzothiophene ring system resulted in analogues **55** and **56**. The FPT inhibitory potency determined for these compounds clearly suggests that the 5,6-fusion is preferred relative to 6,7-

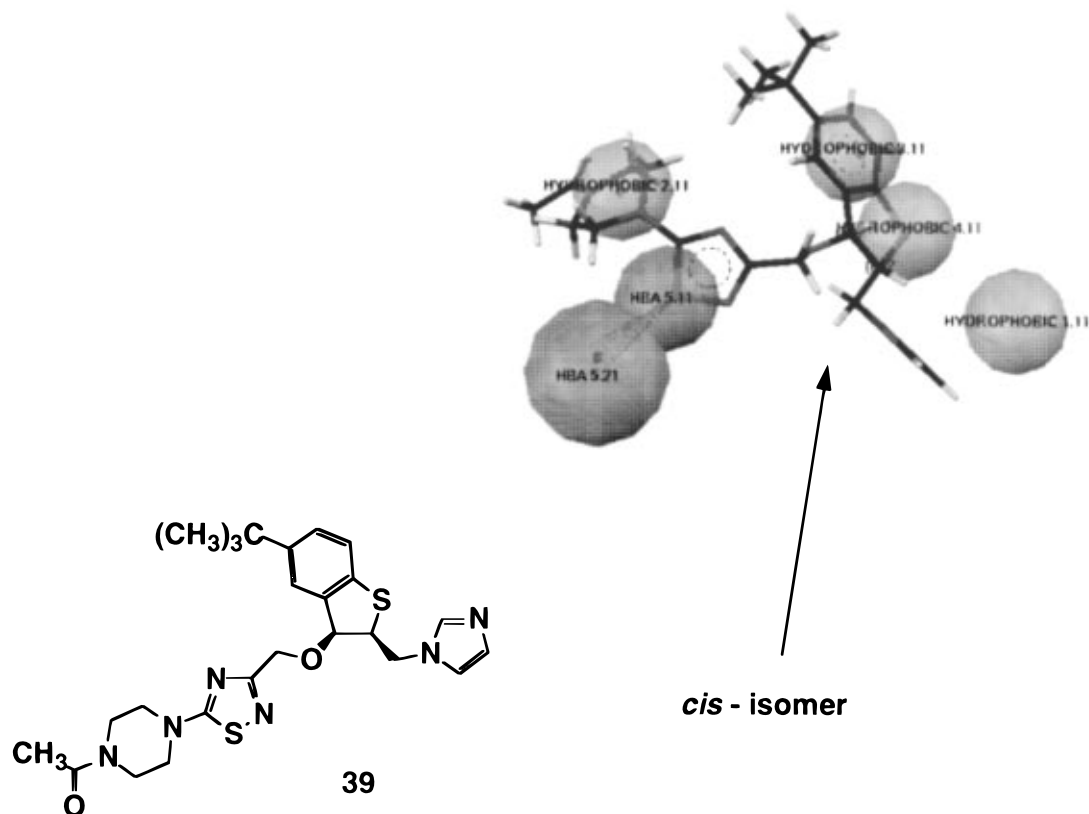


Figure 6. Best conformation of **39**, *cis*-isomer, flexibility fit to the lowest cost catalyst generated FPT hypothesis.

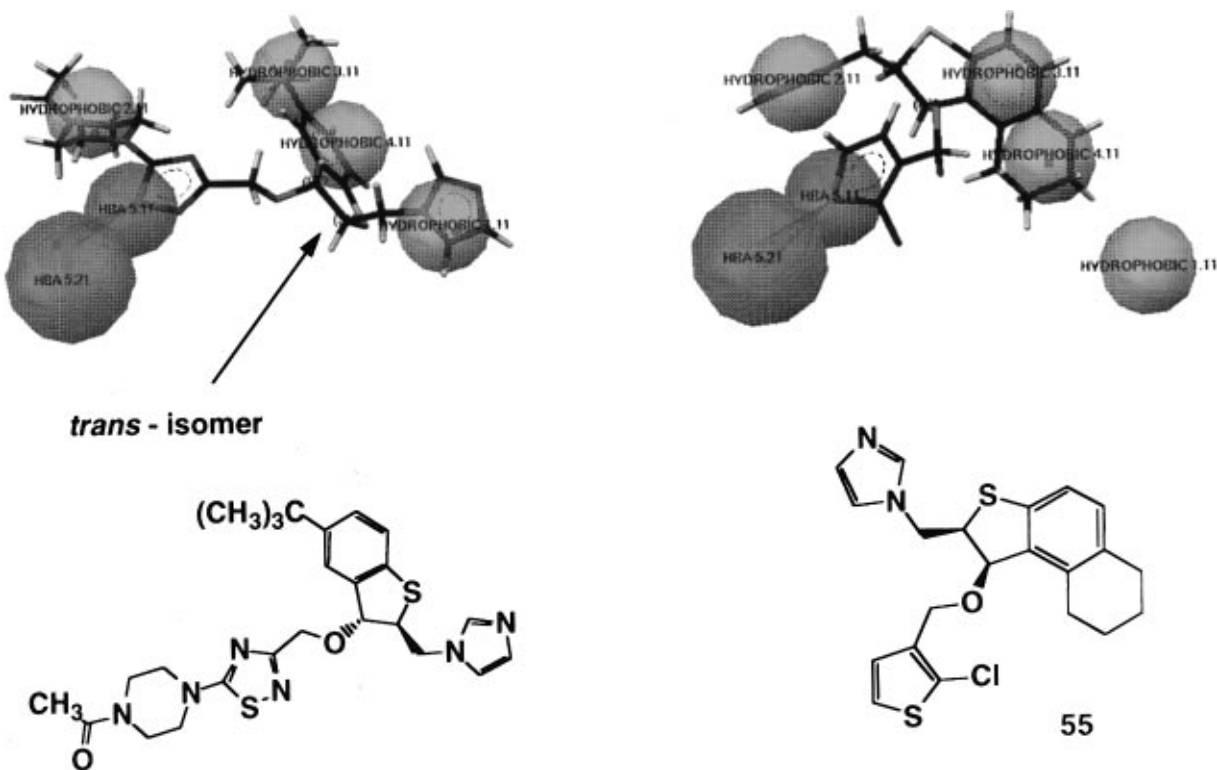


Figure 7. A conformation of the *trans*-isomer of **39** and the best conformation of **55** flexibility fit to the lowest cost catalyst generated FPT hypothesis.

fusion, i.e. **55**, $IC_{50} = 0.2 \mu M$ compared to **56**, $IC_{50} = 10.8 \mu M$. Fusion of an aromatic ring to the 7,8-positions of the dihydrobenzothiophene ring system resulted in analogue **57**. While not directly comparable to either fused aliphatic system, **55** or **56**, the FPT inhibitory

potency of **57**, $IC_{50} = 1.5 \mu M$, is less than that of **55**, but greater than that of **56**.

Oxidation of the sulfur atom in the dihydrobenzothiophene ring system of **44**, $IC_{50} = 2.3 \mu M$, resulted in the sulfinyl analogue **72**, while oxidation of the sulfur

atom in **62**, $IC_{50} = 5.4 \mu\text{M}$, resulted in the sulfonyl analogue **73**. Both of the sulfur-oxidized analogues were less potent FPT inhibitors relative to their unoxidized counterparts, i.e. **72**, $IC_{50} = 20.8 \mu\text{M}$, and **73**, $IC_{50} = 45.9 \mu\text{M}$.

The structure–FPT inhibitory activity relationships determined from the preliminary study described above are summarized in Figure 5, and the most active FPT inhibitors identified from the initial leads, were **55** and **60**, Table 2. While the FPT inhibitory potency of **55**, $FPT IC_{50} = 0.2 \mu\text{M}$, and GGPT-1, $IC_{50} = 16.8 \mu\text{M}$, and **60**, $FPT IC_{50} = 0.3 \mu\text{M}$, and GGPT-1, $IC_{50} = 0.7 \mu\text{M}$, are comparable to each other, the FPT to GGPT-1 selectivity of **55** (84) is greater than the FPT to GGPT-1 selectivity of **60** (2).

Using one of the initial lead compounds, **39**, as an example, a flexible fit of the cis-isomer of this molecule maps to the lowest cost Catalyst-generated FPT hypothesis as described in Figure 6. Only three of the four possible hydrophobic regions of the FPT hypothesis map to the molecule, i.e. the piperazine ring of the side chain, and the aromatic ring and sulfur atom of the dihydrobenzothiophene ring system. The hydrogen bond acceptor in the generated FPT hypothesis is identified as the sulfur atom in the thiadiazine ring system.¹⁷ The estimated FPT inhibitory activity for the cis-isomer of **39**, $IC_{50} = 3.8 \mu\text{M}$, based on the generated FPT hypothesis is in excellent agreement with its experimentally measured FPT inhibitory activity, $IC_{50} = 4.8 \mu\text{M}$. This observation is particularly surprising since only four of the five features of the FPT hypothesis map to the molecule.

Interestingly, the trans-isomer of **39**, flexibly fit to the lowest cost Catalyst-generated FPT hypothesis, maps to all five features of the hypothesis, Figure 7. More importantly, an estimate of the FPT inhibitory activity of this isomer based on the model, $IC_{50} = 0.18 \mu\text{M}$, suggests that the trans-isomer could be as potent as **55**, the best compound identified from the structure–FPT inhibitory relationship study, $IC_{50} = 0.2 \mu\text{M}$. In addition, the FPT inhibitory potency of **55** might also be improved by further analogue synthesis. Since **55** maps to only four of the five features of the lowest cost Catalyst-generated FPT hypothesis, Figure 7, introduction of functionality in **55** which might interact with the fifth feature of the hypothesis could impart enhanced FPT inhibitory activity to the compound.

Summary

In summary, using a training set of novel farnesyl protein transferase (FPT) inhibitors, exemplified by the prototype 1-(4-pyridylacetyl)-4-(8-chloro-4-(8-chloro-5,6-dihydro-11*H*-benzo[5,6]cyclohepta[1,2-*b*]pyridin-11-ylidene)piperidine, Sch 44342, **1**, a three-dimensional pharmacophore model (hypothesis) was generated which successfully correlated the FPT inhibitory activity observed for this series of these compounds to their chemical structure. Using the lowest cost Catalyst-generated FPT hypothesis as a three-dimensional query to search a database of compounds identified several other structurally novel analogues that exhibited the biological activity of the prototype. Investigating the structure–

FPT inhibitory activity relationships of one of the identified series using the lowest cost Catalyst-generated FPT hypothesis demonstrated that it was useful for assessing the relative merits of proposed synthetic targets prior to their synthesis. In addition, the lowest cost Catalyst-generated FPT hypothesis was useful in the conceptual design of other novel FPT inhibitor targets in the series.

Acknowledgment. We thank Drs. W. Robert Bishop, Joseph Catino, A. K. Ganguly, and Paul Kirschmeier for their support of this effort.

References

- (1) Barbacid, M. ras Genes. *Annu. Rev. Biochem.* **1987**, *56*, 779–827.
- (2) Bourne, H. R.; Sanders, D. A.; McCormick, F. The GTPase Superfamily: A Conserved Switch for Diverse Cell Functions. *Nature (London)* **1990**, *348*, 125–132.
- (3) Hall, A. The Cellular Functions of Small GTP-Binding Proteins. *Science* **1990**, *249*, 635–640.
- (4) Casey, P. J.; Solski, P. A.; Der, C.; Buss, J. E. p21ras is modified by a farnesyl isoprenoid. *Proc. Natl. Acad. Sci. U.S.A.* **1989**, *86*, 8323–8327.
- (5) Zhang, F. L.; Casey, P. J. Protein Prenylation: Molecular Mechanisms and Functional Consequences. *Annu. Rev. Biochem.* **1996**, *65*, 241–269.
- (6) Graham, S. L. Inhibitors of Protein Farnesylation: A New Approach to Cancer Chemotherapy. *Exp. Opin. Ther. Pat.* **1995**, *5*, 1269–1285.
- (7) Sepp-Lorenzino, L.; Ma, Z.; Rands, E.; Kohk, N. E.; Gibbs, J. B.; Oliff, A.; Rosen, N. A Peptidomimetic Inhibitor of Farnesyl: Protein Transferase Blocks the Anchorage-dependent Growth of Human Tumor Cell Lines. *Cancer Res.* **1995**, *55*, 5302–5309.
- (8) Nagasu, T.; Yoshimatsu, K.; Rowell, C.; Lewis, M. D.; Garcia, A. M. Inhibition of Human Tumor Xenograft Growth by Treatment with the Farnesyl Transferase Inhibitor B956. *Cancer Res.* **1995**, *55*, 5310–5314.
- (9) Bishop, W. R.; Bond, R.; Petrin, J.; Wang, L.; Patton, R.; Doll, R.; Njoroge, G.; Catino, J.; Schwartz, J.; Windsor, W.; Sayto, R.; Schwartz, J.; Carr, D.; James, L.; Kirschmeier, P. Novel Tricyclic Inhibitors of Farnesyl Protein Transferase. *J. Biol. Chem.* **1995**, *270*, 30611–30618.
- (10) Mallams, A. K.; Njoroge, F. G.; Doll, R. J.; Snow, M. E.; Kaminski, J. J.; Rossman, R.; Vibulbhan, B.; Bishop, W. R.; Kirschmeier, P.; Liu, M.; Bryant, M. S.; Alvarez, C.; Carr, D.; James, L.; King, I.; Li, Z.; Lin, C.-C.; Nardo, J.; Petrin, J.; Remiszewski, S.; Taveras, A.; Wang, S.; Wong, J.; Catino, J.; Girijavallabhan, V.; Ganguly, A. K. Antitumor 8-Chlorobenzocycloheptapyridines: A New Class of Selective, Nonpeptidic, Nonsulphydryl Inhibitors of Ras Farnesylation. *Bioorg. Med. Chem.* **1997**, *5*, 93–99.
- (11) Njoroge, F. G.; Doll, R. J.; Vibulbhan, B.; Alvarez, C.; Bishop, W. R.; Petrin, J.; Kirschmeier, P.; Carruthers, N. I.; Wong, J. K.; Albanese, M. M.; Piwinski, J. J.; Catino, J.; Girijavallabhan, V.; Ganguly, A. K. Discovery of Novel Nonpeptide Tricyclic Inhibitors of Ras Farnesylation. *Bioorg. Med. Chem.* **1997**, *5*, 101–114.
- (12) Njoroge, F. G.; Vibulbhan, B.; Alvarez, C.; Bishop, W. R.; Petrin, J.; Doll, R. J.; Girijavallabhan, V.; Ganguly, A. K. Novel Tricyclic Aminoacetyl and Sulfonamide Inhibitors of Ras Farnesyl Protein Transferase. *Bioorg. Med. Chem. Lett.* in press.
- (13) Catalyst v2.1. Molecular Simulations, Inc., Burlington, MA.
- (14) Sprague, P. W. Automated Chemical Hypothesis Generation and Database Searching with Catalyst. *Perspect. Drug Discovery Des.* **1995**, *3*, 1–20.
- (15) Rane, D. F.; Pike, R. E.; Puar, M. S.; Wright, J. J.; McPhail, A. T. A Novel Synthesis of Cis-1-[[6-Chloro-3-[(2-chloro-3-thienyl)methoxy]-2,3-dihydrobenzo[*b*]thien-2-yl]methyl]-1*H*-imidazole. A New Class of Azole Antifungal Agents. *Tetrahedron* **1988**, *44*, 2397–2402.
- (16) Casey, P. J.; Thissen, J. A.; Moomaw, J. Enzymatic Modification of Proteins with a Geranyl geranylisoprenoid. *Proc. Natl. Acad. Sci. U.S.A.* **1991**, *88*, 8631–8635.
- (17) Allen, F. H.; Bird, C. M.; Rowland, R. S.; Raithby, P. R. Hydrogen-bond Acceptor and Donor Properties of Divalent Sulfur. *Acta Crystallogr., Sect. B: Struct. Sci.* **1997**, *B53* (4), 696–701.

JM970291V